MONITORING UNSATURATED FLOW AND TRANSPORT USING CROSS-BOREHOLE GEOPHYSICAL METHODS

M. C. LOOMS[1], K. H. JENSEN[1], L. NIELSEN[1], A. BINLEY[2] AND H. THYBO[1]

[1] University of Copenhagen, Institute of Geology, Oester Voldgade 10, DK-1350 Copenhagen K, Denmark [2] Lancaster University, Department of Environmental Science, Lancaster, LA1 4YQ, United Kingdom

ABSTRACT

Non-invasive cross-borehole geophysical methods were applied in the unsaturated zone to measure the temporal and spatial variation of water content and tracer concentration. The obtained results were used to determine important transport parameters, i.e. pore water velocity and longitudinal dispersivity. Measurements were conducted during a 20-day forced infiltration experiment using a saline tracer. One-dimensional profiles of water content and tracer concentration were calculated and examined to elucidate the downward migration and spreading of water and tracer. The results show that layering of the subsurface, having just slight contrasts in grain size, can lead to flow barriers and create lateral flow, mechanisms that influence the water front velocity and transport parameters substantially.

1. INTRODUCTION

Measurements of unsaturated hydraulic properties and monitoring of flow variables and concentration are traditionally based on very small support volumes, typically in the order of 100 cm^3. This scale is generally much smaller than the scale on which these parameters and variables are needed. This could be for an agricultural field (~ 100 m), a grid element in a distributed hydrological model (~ 200 m) or a hydrological catchment (~ km's). Evidently there is a mismatch between measurement scale and application scale. The scale problem is a general problem in hydrology but perhaps most critical for the unsaturated zone due to the non-linearity of the flow processes.

Recent research has shown that cross-borehole geophysical methods offer promising alternatives to traditional techniques for hydrological characterization. The measurements collected by these methods are on a more appropriate scale and with minimum intrusion of the sediment. In particular, cross-borehole Ground Penetrating Radar (GPR) and Electrical Resistivity Tomography (ERT) can provide data on soil moisture content and conductivity variations in the vadose zone between boreholes located up to ~10 m apart [*Alumbaugh et al.* 2002; *Binley et al.* 2002; *Daily et al.* 1992, *Ferré et al.* 2003]. Such data may serve as input to inversion models for identification of hydraulic and transport parameters.

This paper describes cross-borehole ERT and GPR measurements conducted simultaneously at a field site during a water and tracer infiltration experiment. Variations in fluid conductivity, and thereby tracer concentration, were obtained by combining the water content profiles from cross-borehole GPR with the bulk conductivity profiles achieved from cross-borehole ERT [*Binley et al.* in press]. The obtained water content and concentration

profiles were subsequently used for identification of flow and transport characteristics in the form of water front velocity, pore water velocity and longitudinal dispersivity.

2. FIELD SITE

The field site was established in Denmark on a 20 – 30 m layer of unsaturated melt water sand. A schematic of the field site setup is illustrated in Figure 1. The experimental setup consists of four ERT and four GPR boreholes drilled to a depth of 12 m. The 8 boreholes form a cross consisting of two lines. Along each line, the outer two boreholes (7 m apart) are equipped with ERT instrumented PVC-tubes (electrodes every 50 cm) while the inner two boreholes (5 m apart) have access tubes for GPR antennae.

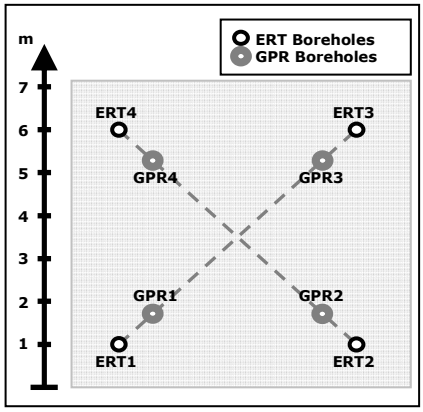

FIGURE 1. Schematic of the field site setup. The light grey area is the infiltration area.

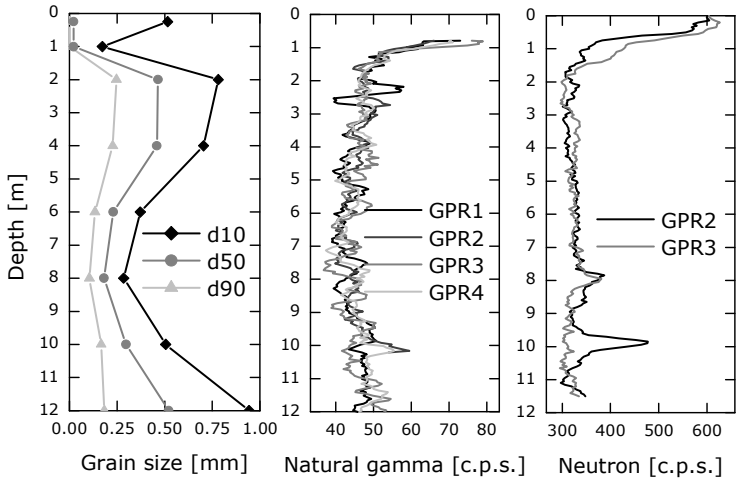

FIGURE 2. (a) Sediment samples from a nearby well. d10, d50 and d90 are the 10th, 50th and 90th percentile of the grain size distribution. Data is provided by Copenhagen Energy. (b & c) Well logs conducted at the field site. GPR1, 2, 3 and 4 refer to the GPR boreholes in Figure 1.

Figure 2(b) and (c) present well logging results (natural gamma and neutron logging) collected in the GPR access tubes. The subsurface appears not to vary substantially with depth. However, the results of a grain size analysis of sediment samples taken at a nearby well, Figure 2(a), indicate that a slight layering exists. The grain size percentiles show that the

top 1 m consists mainly of silt, with just a small fraction of clay. Below this top soil a layered sequence can be observed. Coarse sand, followed by finer sand and finally coarse sand again.

3. EXPERIMENTAL PROCEDURE

A forced tracer infiltration experiment was initiated at the field site in October 2005. Cross-borehole GPR (measuring moisture content) and cross-borehole ERT (measuring resistivity) were used to monitor the downward migration of water and tracer.

3.1 Cross-borehole GPR

Measurements were taken using a Sensors and Software PulseEKKO PE100 system equipped with 100 MHz antennae. A Zero Offset Profiling (ZOP) technique was used, whereby the one-dimensional electromagnetic wave velocity distribution between two boreholes was estimated. Two antennae were lowered simultaneously into a set of boreholes stopping every 0.25 m to take a measurement. A total of six ZOP were collected using all possible sets of pairs between the four boreholes on Figure 1, i.e. GPR1–2, GPR1–3, GPR1–4, GPR2–3, GPR2–4, and GPR3–4. The first arrival time of each electromagnetic wave was picked individually and the resulting velocity of each position was converted to dielectric constant and moisture content using:

$$\sqrt{\varepsilon_r} = \frac{c}{v} \tag{1}$$

and the empirical relationship of Topp et al. (1980):

$$\theta = -5.3*10^{-2} + 2.92*10^{-2}\varepsilon_r - 5.5*10^{-4}\varepsilon_r^{\,2} + 4.3*10^{-6}\varepsilon_r^{\,3} \tag{2}$$

where v is the resulting velocity, c the radar wave velocity in air (≈ 0.3 m/ns), ε_r the bulk dielectric constant, and θ the moisture content at a given depth.

3.2 Cross-borehole ERT

Prior to initiating the experiment, 96 electrodes were installed in the field: 84 borehole electrodes and 12 surface electrodes. The latter were set up along the dotted lines on Figure 1 with 1 m spacing. Four electrodes were used for each resistance measurement. A measurement scheme, consisting of 2315 measurements and 2315 reciprocals, was constructed using only horizontal borehole dipoles [*Rubin and Hubbard*, 2005]. In the reciprocal measurements the current and potential electrodes used in the original measurements were interchanged. An IRIS SYSCAL Pro Switch 96 10-channel system was used resulting in a 2 hrs 15 min sampling period. Only data having a reciprocal error < 10% (1767 measurements) was used in the final data inversion [*LaBrecque et al.* 1996; *Slater et al.* 2000]. The Occam based Lancaster 3-D resistivity inversion program, R3, was utilized for this purpose, producing three-dimensional resistivity tomograms. The obtained bulk resistivity, ρ_b, is by Archie's empirical law (Archie, 1942) related to the pore water resistivity, ρ_w, the porosity, Φ, and the saturation degree, S = θ/Φ:

$$\rho_b = \rho_w \Phi^{-m} S^{-n} \tag{3}$$

where *m* and *n* are empirical constants typically set to 1.3 and 2, respectively, but dependent on the soil in question.

By isolating the pore water resistivity from Equation 3:

$$\rho_w = \frac{\theta^n \rho_b}{\Phi^{(n-m)}} \tag{4}$$

the pore water resistivity, ρ_w, can be found using the bulk resistivity determined by cross-borehole ERT, the moisture content, θ, determined from cross-borehole GPR and an assumed constant and known porosity.

3.3 Infiltration experiment

The forced infiltration tracer experiment lasted 20 days from October 18 to November 7, 2005. During 20 days clean water was irrigated at a rate of 88.4 mm/day over a 7.33 m × 7.33 m area using drippers spaced every 33cm over the entire surface (484 drippers). Each dripper consisted of 85 cm long 1 mm tubing having enough resistance to ensure constant flow in all drippers. Measurements were taken on a daily basis at the start of the experiment and reduced to every 2 – 3 days towards the end. After 4 days of infiltration, a saline tracer, 890 L with a conductivity of 105.4 mS/cm, was added over 150 min through the drippers. The infiltration experiment was designed to mimic one-dimensional water and solute infiltration within the measurement area to enable a simple one-dimensional analysis of the results.

4. RESULTS

Figure 3 shows the background (pre-tracer and pre-infiltration) cross-borehole GPR and ERT moisture content profiles. The GPR profile is an average of the six collected ZOP, while the ERT profile is an average of the infiltration volume contained within the ERT boreholes. As expected, both methods result in moisture profiles having similar trends and magnitude. However, the ERT profile indicates slightly higher moisture contents near the surface and lower moisture contents below approximately 8 m. The vertical resolution of the ERT method is lower than the GPR data, and slight variations in moisture caused by layering will not, as a result, be as pronounced.

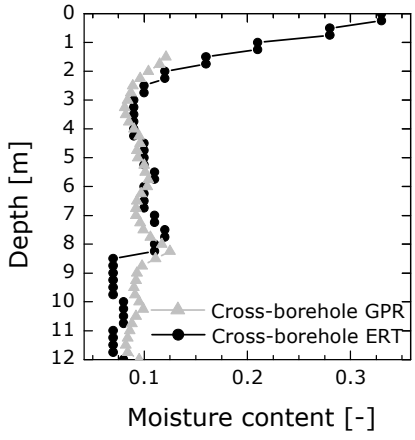

FIGURE 3. Moisture content profiles collected using cross-borehole ERT and GPR.

The GPR data from 0.00 m – 1.50 m is not included in Figure 3. In this region the first arriving electromagnetic signal is a refracted wave and not the direct wave needed to calculate moisture content.

4.1 Soil moisture content profiles

The GPR moisture content profiles collected throughout the infiltration experiment, c.f. Figure 4, elucidate the downward water movement. It is observed in Figure 4 that during the first 7 days of infiltration the water front migrates 0.50 m/day – 1.50 m/day. After approximately 7 days the infiltrating water reaches 8.25 m where further migration is temporarily halted. For the next 6 days, an increase in moisture content above the 8.25 m boundary is observed instead. However, at some time, between Day 13 and Day 15, the water continues the downward movement.

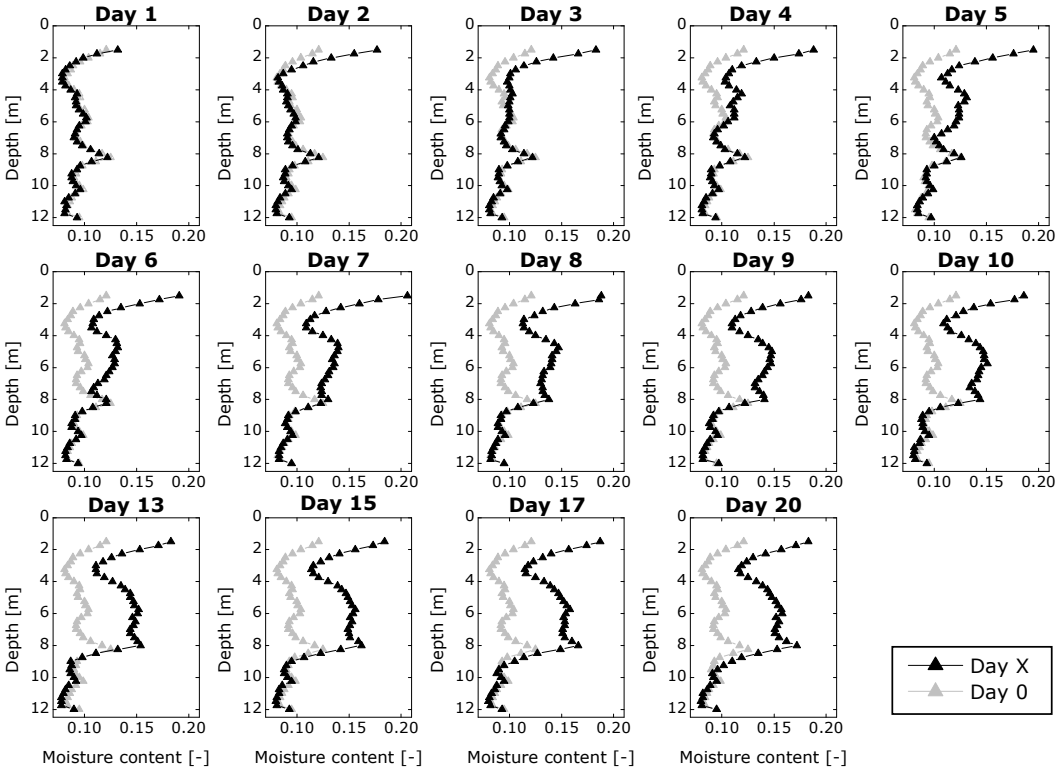

FIGURE 4. Average moisture content profiles measured at various days. The grey curve is the background moisture content profile, i.e. Day 0, also shown in Figure 3.

The collected GPR moisture data can also be plotted as water breakthrough curves, Figure 5(a). Furthermore, the data can be used to evaluate the amount of water accumulated within the measurement volume, Figure 5(b). This figure clearly shows how the amount of infiltrated water is constant during the first 6 – 7 days. After 7 days the water accumulation stagnates coinciding with the time the water front reaches 8.25 m. The sediment at 8 m depth has the lowest grain sizes throughout the profile and overlays coarser material, c.f. Figure 2(a). A capillary barrier appears to be created at this depth. The water builds up above the capillary barrier and at the same time lateral transport out of the infiltration area takes place. This continues until the moisture content becomes great enough (the matric potential low enough) for the water to penetrate into the underlying coarser sand. After 13 days, the water breaks through the capillary barrier and the water accumulated in the measurement volume increases again.

The rate of water accumulated in the measurement volume, 2.32 m^3/day, differs by over a factor 2 with the rate of water infiltrated through the drippers; 4.75 m^3/day. The difference

between these two infiltration rates is quite substantial. Therefore it is felt that erroneous moisture content estimates due to refraction or inadequate petrophysical relationships cannot fully explain the disagreement. Lateral flow above 1.50 m and a consequently larger infiltration area can perhaps better explain the large quantities of missing water.

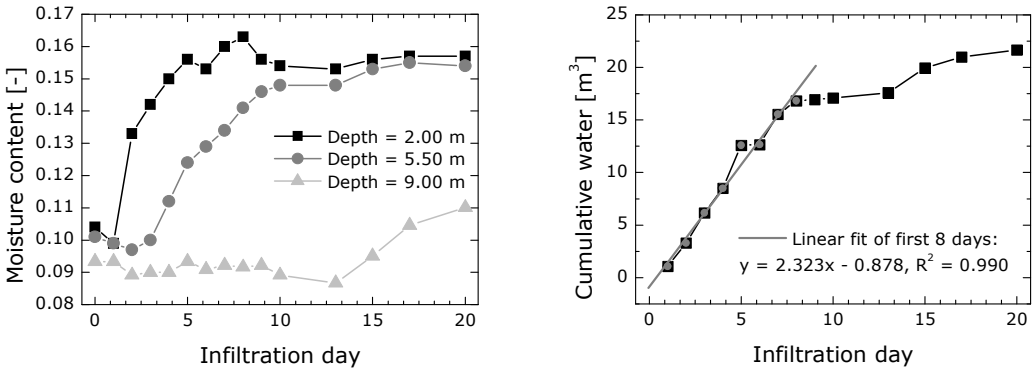

FIGURE 5. (a) Moisture breakthrough curves at three different depths. (b) Cumulative difference in water volume for entire infiltration area.

4.2 Resistivity profiles

The ERT bulk resistivity values, averaged at each depth to represent a 1D-profile, are plotted in Figure 6.

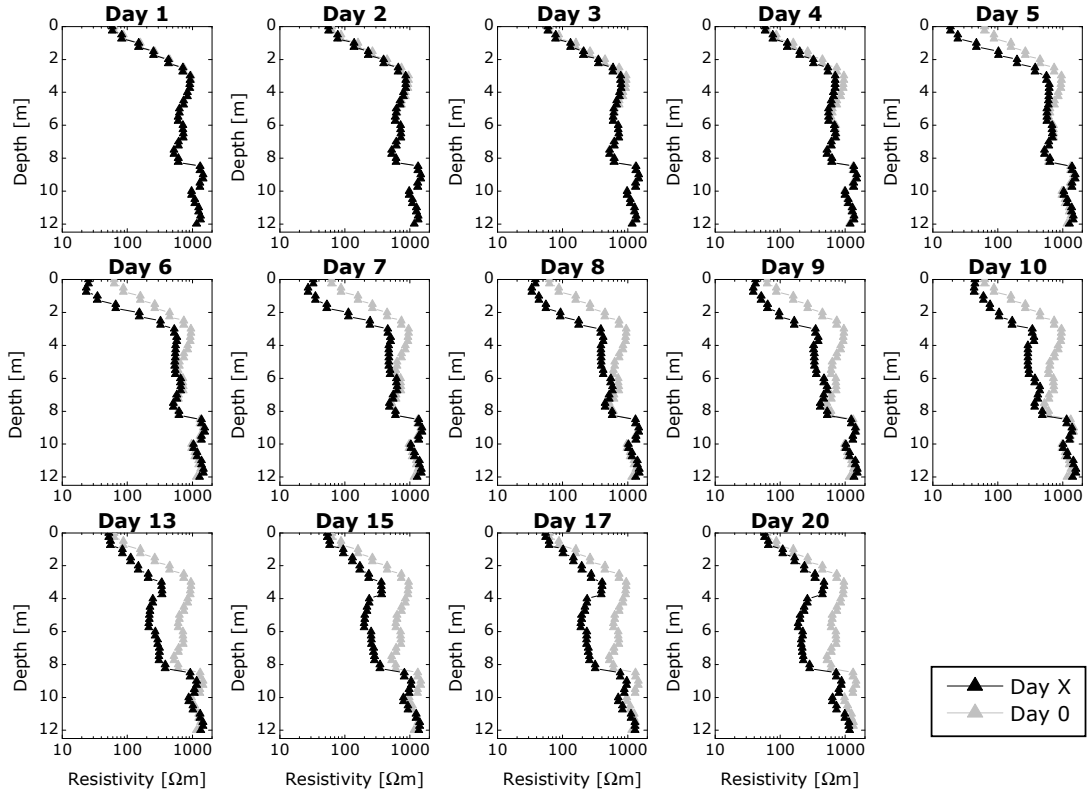

FIGURE 6. Average resistivity profiles measured at various days. The grey curve is the background resistivity profile, i.e. Day 0.

Figure 6 shows how the water infiltration during the first 4 days only lowers the resistivity slightly near the top of the profile. However, there is a clear reduction in resistivity (an increase in conductivity) after 5 days, corresponding to the time the tracer is added. The subsequent 9 profiles illustrate the tracer's downward movement and the spreading of tracer.

4.3 Tracer profiles and moment analysis

The tracer movement and spreading is, however, much more pronounced when the cross-borehole ERT and GPR results are combined to calculate the tracer concentration see Figure 7. The tracer pulse is very distinct from Day 5 to Day 10, illustrating clearly how the centre of mass slowly migrates down through the subsurface. The pulse has, at Day 13, dispersed considerably, and after Day 15 it is difficult to distinguish the tracer and the centre of mass.

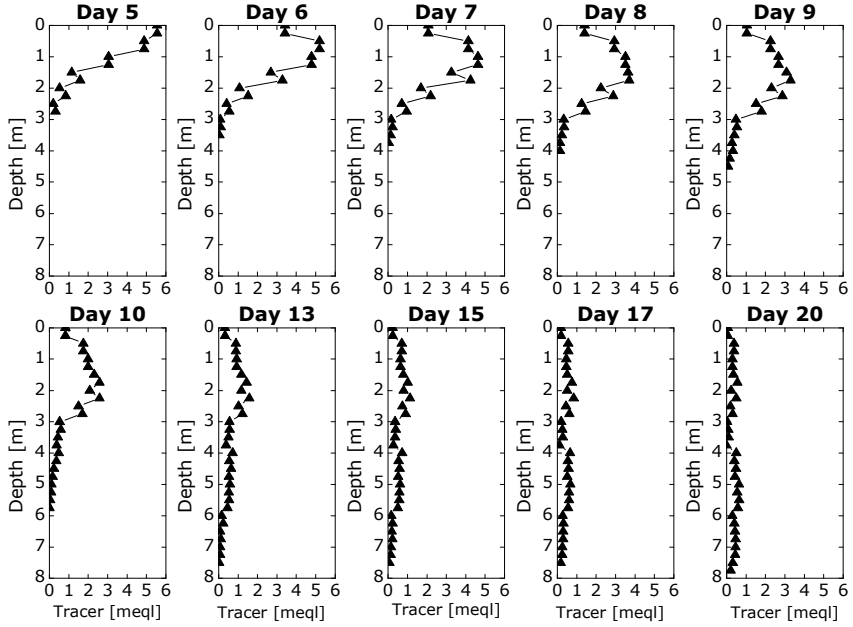

FIGURE 7. Average tracer mass profiles calculated for various days.

The mass profiles in Figure 7 were used for moment analysis. The results of this analysis are listed in Table 1. They reveal a temporal development of the transport parameters. The pore water velocity of the tracer declines throughout the measurement period, decreasing most substantially during the first four to five days. After 5 days the pore water velocity stabilizes at approximately 0.3 m/day. As expected, the magnitude of the estimated pore water velocity is lower than the water front velocity.

The dispersivity values are low, around 0.2 m, for the first five days and increase to 0.5 m during the last period of the infiltration experiment. The changes in both pore water velocity and dispersivity coincide with the standstill of the water front at approximately 8 m. At about the same time, a serious lack of mass is observed, see Table 1. This indicates that the assumption regarding one-dimensional vertical flow is being violated by water flowing laterally out of the infiltration area.

The amount of mass distributed on the area was 17.3 meql. This amount is double the amount of mass measured using the cross-borehole geophysical techniques, see Table 1. The lack of mass is in accordance with the previously discussed water error, and confirms the speculation that tracer and water moves laterally out of the measurement area.

TABLE 1. Water front velocity and moment analysis results.

	Water infiltration	Tracer		
	Water front velocity [m/day]	Mass [meql]	Pore water velocity [m/day]	Dispersivity, α_L [m]
Day 1	1.25	-	-	-
Day 2	1.00	-	-	-
Day 3	1.00	-	-	-
Day 4	1.00	-	-	-
Day 5	1.25	7.21	0.80	0.24
Day 6	1.50	8.71	0.53	0.21
Day 7	0.50	8.57	0.42	0.20
Day 8	0.25	7.83	0.37	0.21
Day 9	0.00	7.15	0.33	0.24
Day 10	0.00	6.24	0.31	0.31
Day 13	0.00	4.77	0.31	0.50
Day 15	0.75	3.92	0.28	0.55
Day 17	0.50	3.36	0.27	0.57
Day 20	0.25	2.77	0.27	0.55

5. DISCUSSION AND CONCLUSIONS

Cross-borehole ERT and GPR provide a novel and promising alternative to existing methodologies designed to monitor tracer infiltration. We have demonstrated that when both cross-borehole methods are combined tracer mass profiles can be obtained. These profiles enable a determination of important transport parameters through moment analysis. The findings in this work does, however, underline that even small structural changes in layered sediments can result in capillary barriers and subsequent lateral flow.

REFERENCES

Alumbaugh, D., P. Y. Chang, L. Paprocki, J. R. Brainard, R. J. Glass, and C. A. Rautman (2002), Estimating moisture contents in the vadose zone using cross-borehole ground penetrating radar: A study of accuracy and repeatability, *Water Resources Research, 38(12)*, 1309, doi:10.1029/2001WR000754.

Binley, A., G. Cassiani, R. Middleton, and P. Winship (2002), Vadose zone flow model parameterisation using cross-borehole radar and resistivity imaging, *Journal of Hydrology*, *267*, 147–159.

Binley, A., P. Winship, and D. Gomez, Flow and transport in the unsaturated Sherwood sandstone: Characterization using cross-borehole geophysical methods, in press.

Copenhagen Energy, Water Department, Section for Water Quality

Daily, W., A. Ramirez, D. LaBrecque, and J. Nitao (1992), Electrical resistivity tomography of vadose water movement, *Water Resources Research, 28(5)*, 1429–1442.

Ferré, T. P. A., G. von Glinski, and L. A. Ferré (2003), Monitoring the maximum depth of drainage in response to pumping using borehole ground penetrating radar, *Vadose Zone Journal*, *2*, 511–518.

LaBrecque, D. J., M. Miletto, W. Daily, Ramirez, A., and E. Owen (1996), The effects of noise on Occam's inversion of resistivity tomography data, *Geophysics, 61(2)*, 538–548.

Rubin, Y. and S. S. Hubbard (Eds.) (2005), *Hydrogeophysics*. 523 pp., Water Science and Technology Library, vol. 50, Springer, The Netherlands.

Slater, L., A. M. Binley, W. Daily, and R. Johnson (2000), Cross-hole electrical imaging of a controlled saline tracer injection, *Journal of Applied Geophysics, 44*, 85–102.